Electronic supplementary information (ESI†)

A comparative study of optical nonlinearities of *trans*- A_2B-corroles in solution and in aggregated State

Antara Garai,[a] Samir Kumar, [b] Woormileela Sinha, [a] Chandra Shekhar Purohit, [a] Ritwick Das*, [b] and Sanjib Kar*, [a]

[a]*School of Chemical Sciences, National Institute of Science Education and Research (NISER), Bhubaneswar – 751005, India.*

[b]*School of Physical Sciences, National Institute of Science Education and Research (NISER), Bhubaneswar – 751005, India.*

E-mail: ritwick.das@niser.ac.in and sanjib@niser.ac.in

Computational details: All the calculations were performed with the program package TURBOMOLE 6.4 using density functional theory (DFT).[1, 2] The BP86 functional and TZVP basis set together with the resolution-of-the-identity (RI) approximation[3-5] (RI-BP86/TZVP in short) was employed for the structure optimization procedure. Numerical frequency calculations of the optimized structures were done to ensure that the optimized structures were true minima not the transition states.

1. Ahlrichs, R.; Baer, M.; Haeser, M.; Horn, H.; Koelmel, C., Electronic structure calculations on workstation computers: the program system TURBOMOLE. *Chem. Phys. Lett.* **1989,** *162*, 165-9.
2. Treutler, O.; Ahlrichs, R., Efficient molecular numerical integration schemes. *J. Chem. Phys.* **1995,** *102*, 346-54.
3. Vahtras, O.; Almloef, J.; Feyereisen, M. W., Integral approximations for LCAO-SCF calculations. *Chem. Phys. Lett.* **1993,** *213* , 514-18.
4. Eichkorn, K.; Treutler, O.; Oehm, H.; Haeser, M.; Ahlrichs, R., Auxiliary basis sets to approximate Coulomb potentials. *Chem. Phys. Lett.* **1995,** *242*, 652-60.
5. Eichkorn, K.; Treutler, O.; Oehm, H.; Haeser, M.; Ahlrichs, R., Auxiliary basis sets to approximate Coulomb potentials. *Chem. Phys. Lett.* **1995,** *240*, 283-90.

Aggregation properties of 3: The aggregates of **3** were prepared by mixing 1 mL of water to a 1 mL DMF solution of **3** (2.04×10^{-5} M) with constant stirring at room temperature (298K). **3** in a 1:1 DMF and H_2O mixture (mole fraction of DMF was ~0.2) shows a Soret band at around 412 nm (Fig. S21). A time dependent profile of UV-Vis spectra was recorded for **3** in a 1:1 DMF and H_2O mixture. Absorbance spectra were recorded on 10 minutes interval (Fig. S21). With the progression of time the Soret band of corrole, **3,** decreases in intensity, however a new band at around 503 nm grows slowly. In addition to this new band, the intensity of the Q-band also slightly increases. A significant red shift of the Q band was observed in the UV-Visible spectra of **3** in a 1:1 mixture of DMF and H_2O in comparison to the spectra of **3** in the pure toluene solvent. A new band at around 724 nm also appears. As per the previous literature, these changes in UV-Vis spectra suggest the formation of aggregates.[1] The formation of aggregates in binary solvent mixture for porphyrin related derivatives is not uncommon.[1] The dynamic light scattering experiment (DLS) of these solutions was performed to measure the size distribution of these aggregates (Fig. S22). A time dependent profile of DLS measurement was also done on 10 minutes interval. However it was observed that the size of the aggregates does not change significantly with the progression of time. Average size distribution of the aggregates was observed in the range of 390-410 nm.

1. (a) O. Valdes-Aguilera and D. C. Neckers, *Acc. Chem. Res.* 1989, **22**, 171; (b) P. R. Ojeda, I. A. K. Amashta, J. R. Ochoa and I. L. Arbeloa, *J. Chem. Soc. Faraday Trans. 2*, 1988, **84**, 1; (c) J. Hessemann, *J. Am. Chem. Soc.* 1980, **102**, 2167; (d) W. Mooney, P. E. Brown, J. C. Russel, S. B. Costa, L. G. Pederson and D. G. Whitten, *J. Am. Chem. Soc.,* 1984, **106**, 5659; (e) W. F. Mooney and D. G. Whitten, *J. Am. Chem. Soc.* 1986, **108**, 5712; (f) H. Fidder, J. Terpstra and D. A. Wiersma, *J. Chem. Phys.* 1991, **94**, 6895; (g) W. West and B. H. Carroll, *The Theory of Photographic Processes*, 3rd ed., T. H. James, Ed., The McMillan Company: New York, 1966; Chapter 12; (h) M. Furuki, K. Ageishi, S. Kim, I. Ando and L. S. Pu, *Thin Solid Films,* 1989, **180**, 193; (i) Y.-w. Jun, J.-s. Choi and J. Cheon, *Angew. Chem., Int. Ed.,* 2006, **45**, 3414; (j) A. Agostiano, P. Cosma, M. Trotta, L. Monsù –Scolaro and N. Micali, *J. Phys. Chem. B,* 2002, **106**, 12820; (k) S. Boussaad, J. A. DeRose and R. M. Leblanc, *Chem. Phys. Lett.* 1995, **246**, 107.

Figure S1. Z-scan experimental set-up using Yb-fiber laser source; FI: Fiber laser; HWP:Half-wave plate; PBS: Polarizing beam-splitter; L: Lens (f =100 mm); TS: Translation stage (10 cm travel; S: Sample; A: Aperture (S ~ 0.3); PD1: Reference photodetector; PD2: Signal photodetector

Figure S2. ^{1}H NMR spectrum of 2,2'-((2-bromo-5-fluorophenyl)methylene)bis(1H-pyrrole) in $CDCl_3$.

Figure S3. ESI- MS spectrum of 2,2'-((2-bromo-5-fluorophenyl)methylene)bis(1H-pyrrole) in CH_3CN shows the measured spectrum with isotopic distribution pattern.

Figure S4. ^{1}H NMR spectrum of 5,10,15-Tris[3,4-(1,4-dioxan)phenyl]corrole, **1** in $CDCl_3$.

Figure S5. ESI- MS spectrum of 5,10,15-Tris[3,4-(1,4-dioxan)phenyl]corrole, **1** in CH_3CN shows the measured spectrum with isotopic distribution pattern.

Figure S6. Fluorescence decay profiles of (a) **1**, (———); λem = 676 nm, (b) **2**, (———); λem = 654 nm, and (c) **3**, (———); λem = 661 nm. The black line represents experimental data, whereas the red line represents best fit.

Figure S7. ^{1}H NMR spectrum of 10-[4-(chloroacetoxy)phenyl]-5,15-bis(2-bromo-5-fluorophenyl) corrole, **2**, in $CDCl_3$.

Figure S8. ^{13}C NMR spectrum of 10-[4-(chloroacetoxy)phenyl]-5,15-bis(2-bromo-5-fluorophenyl) corrole, **2**, in $CDCl_3$.

Figure S9. ESI- MS spectrum of 10-[4-(chloroacetoxy)phenyl]-5,15-bis(2-bromo-5-fluorophenyl) corrole, **2**, in CH_3CN shows the measured spectrum with isotopic distribution pattern.

Figure S10. ^{1}H NMR spectrum of 10-(4-hydroxyphenyl)-5,15-bis(2-bromo-5-fluorophenyl) corrole, **3** in $CDCl_3$.

Figure S11. ^{13}C NMR spectrum of 10-(4-hydroxyphenyl)-5,15-bis(2-bromo-5-fluorophenyl) corrole, **3** in $CDCl_3$.

Figure S12. ESI- MS spectrum of 10-(4-hydroxyphenyl)-5,15-bis(2-bromo-5-fluorophenyl) corrole, **3** in CH_3CN shows the measured spectrum with isotopic distribution pattern.

Figure S13. X-ray single crystal structure analysis of 10-(4-hydroxyphenyl)-5,15-bis(2-bromo-5-fluorophenyl) corrole, **3**, (a) O─H...N interactions, [2.86 Å] (b) π- π stacking interactions [3.51 Å]. The entries in square brackets are the distances. (c)

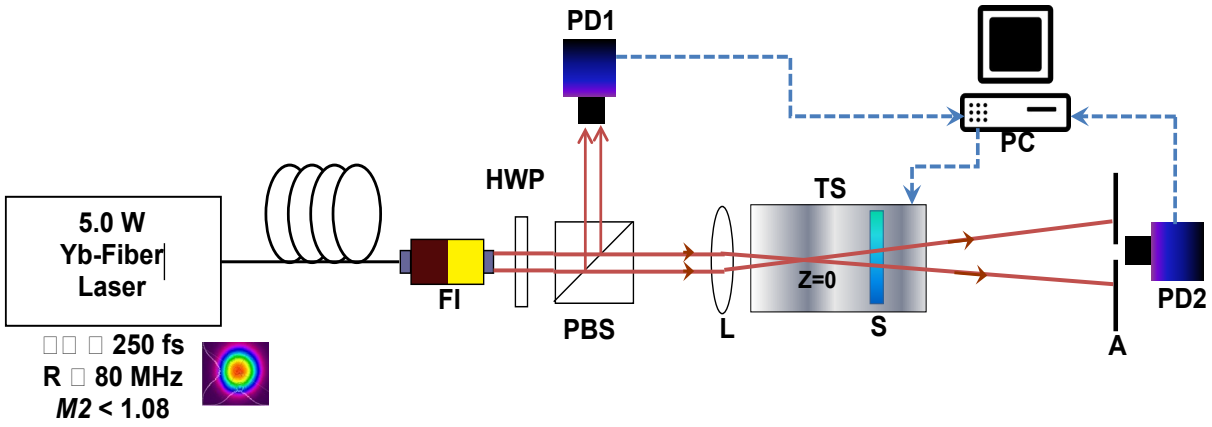

Figure S1. Z-scan experimental set-up using Yb-fiber laser source; FI: Fiber laser; HWP:Half-wave plate; PBS: Polarizing beam-splitter; L: Lens (f =100 mm); TS: Translation stage (10 cm travel; S: Sample; A: Aperture (S ~ 0.3); PD1: Reference photodetector; PD2: Signal photodetector

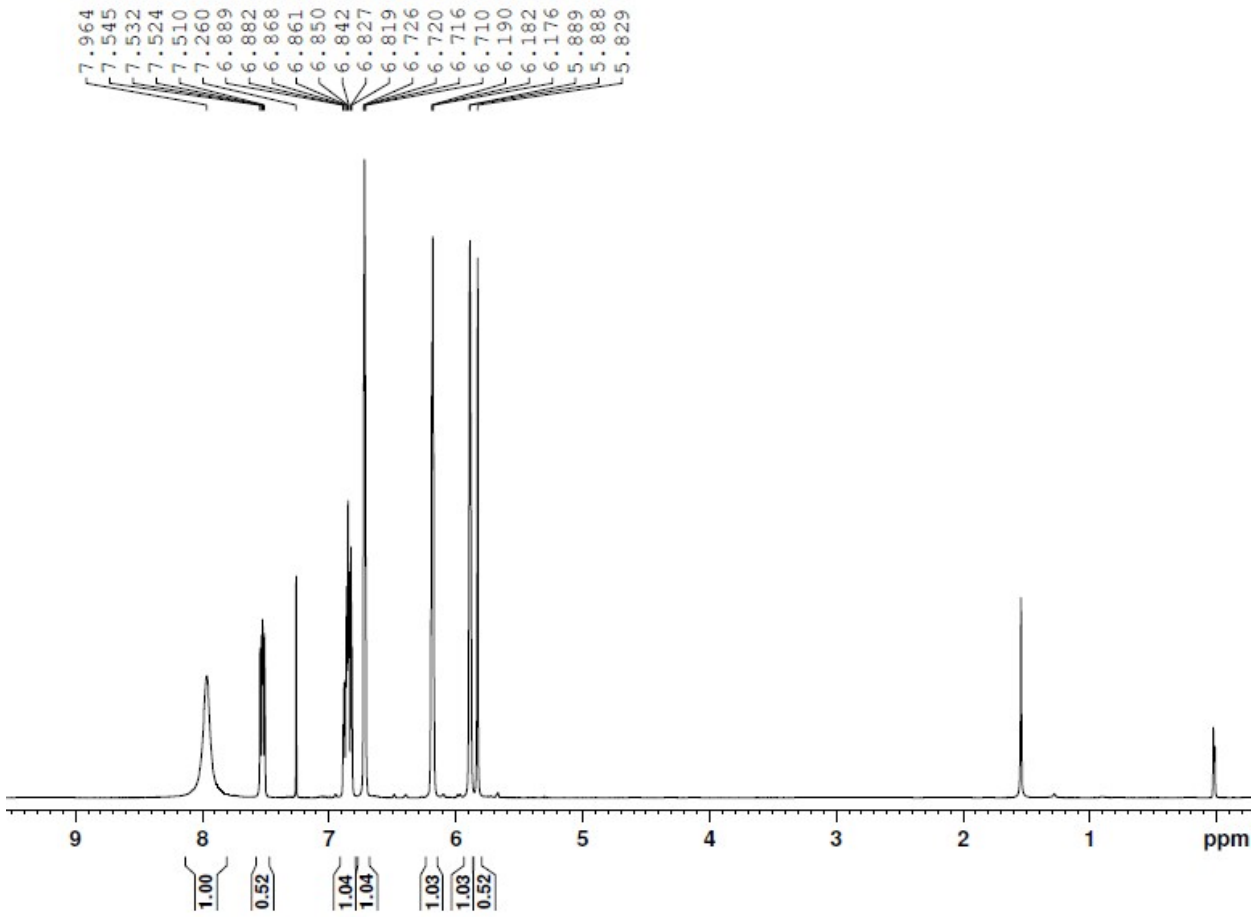

Figure S2. ^{1}H NMR spectrum of 2,2'-((2-bromo-5-fluorophenyl)methylene)bis(1H-pyrrole) in $CDCl_3$.

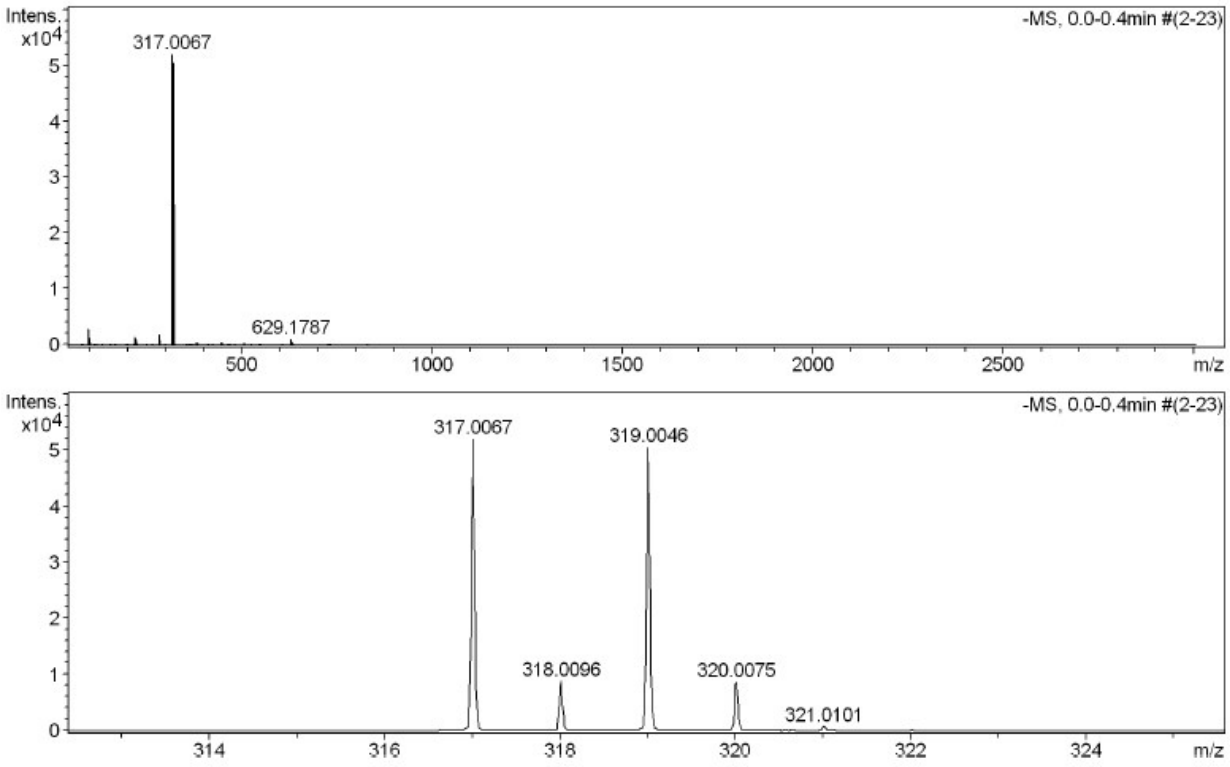

Figure S3. ESI- MS spectrum of 2,2'-((2-bromo-5-fluorophenyl)methylene)bis(1H-pyrrole) in CH_3CN shows the measured spectrum with isotopic distribution pattern.

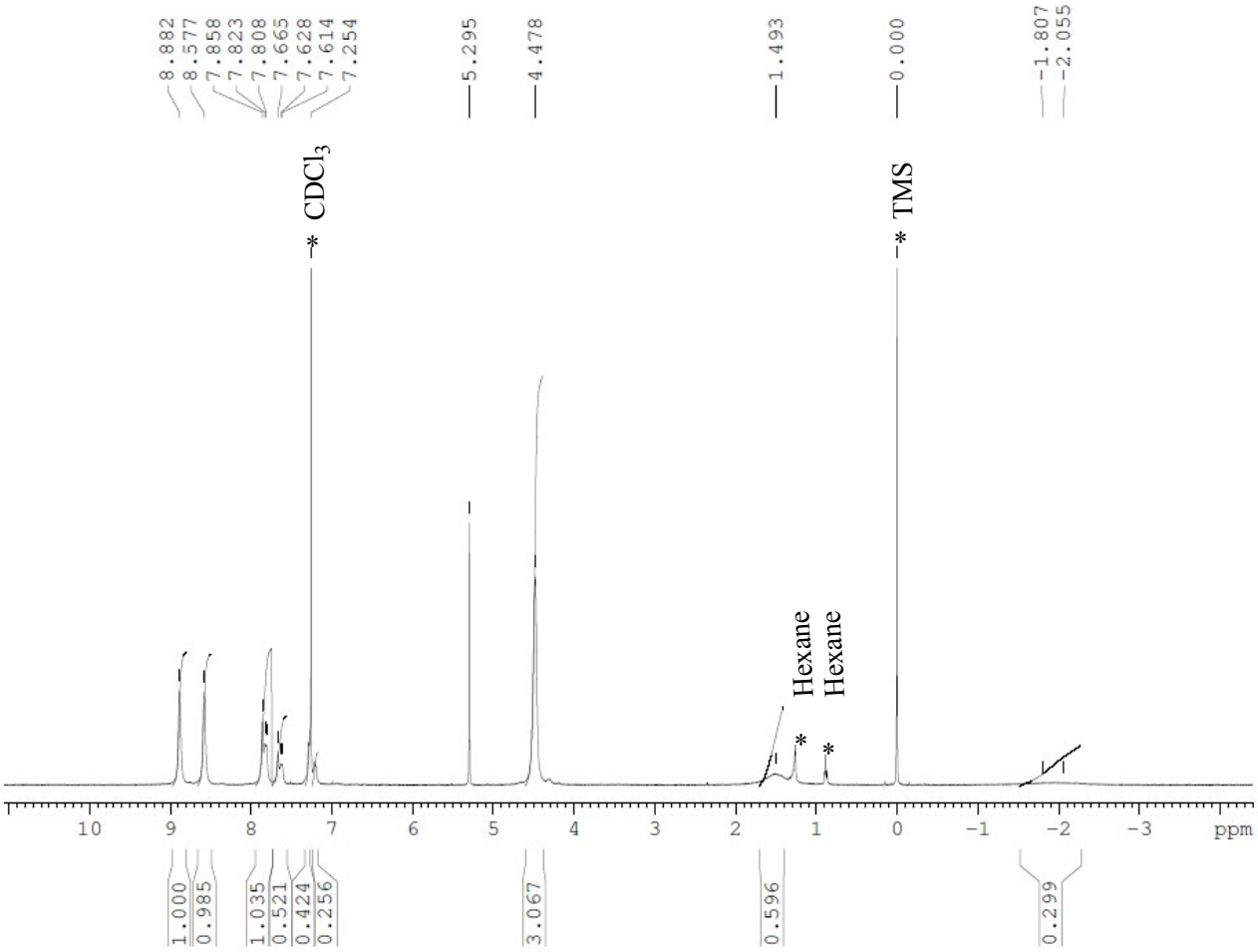

Figure S4. ^{1}H NMR spectrum of 5,10,15-Tris[3,4-(1,4-dioxan)phenyl]corrole, **1** in $CDCl_3$.

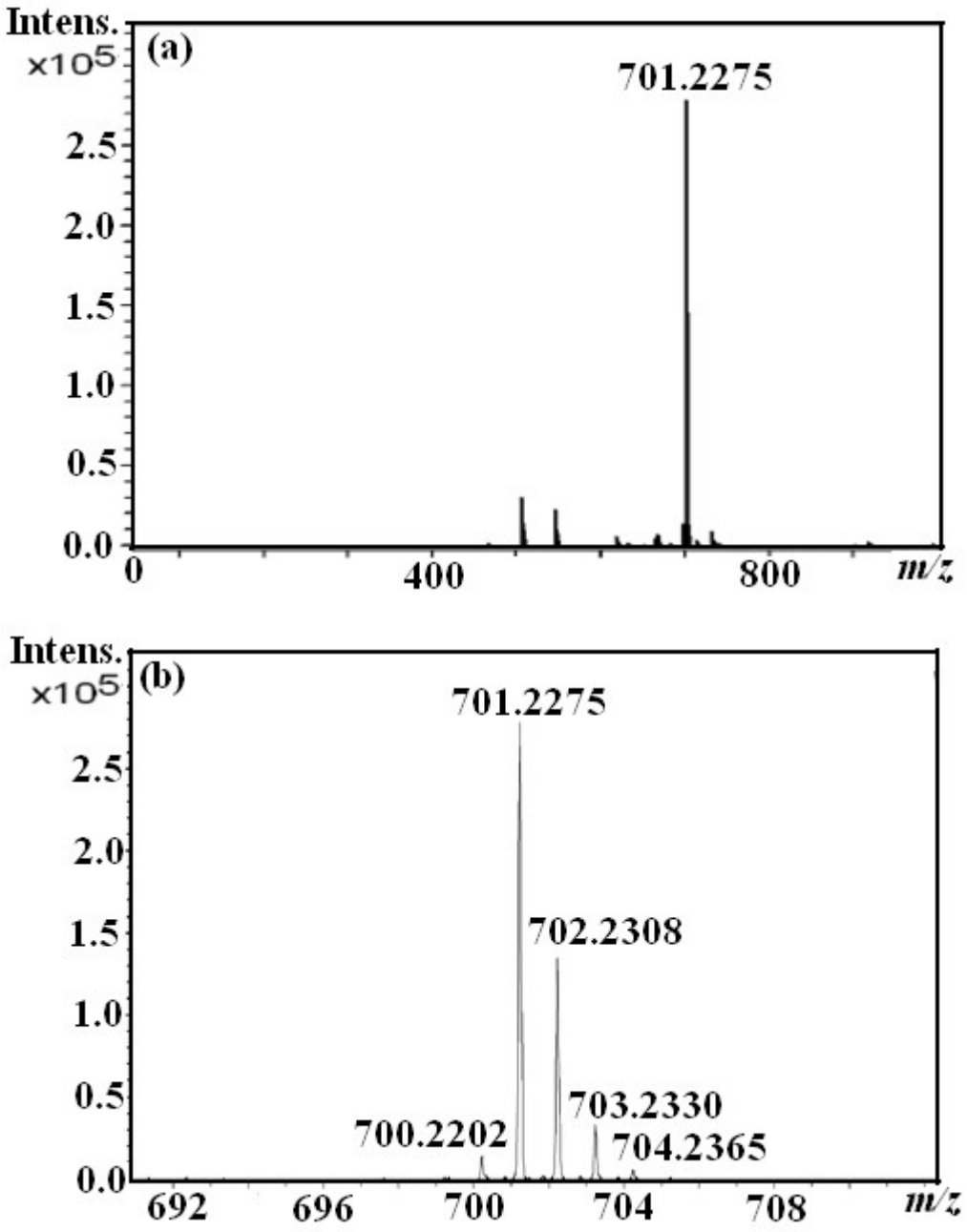

Figure S5. ESI- MS spectrum of 5,10,15-Tris[3,4-(1,4-dioxan)phenyl]corrole, **1** in CH_3CN shows the measured spectrum with isotopic distribution pattern.

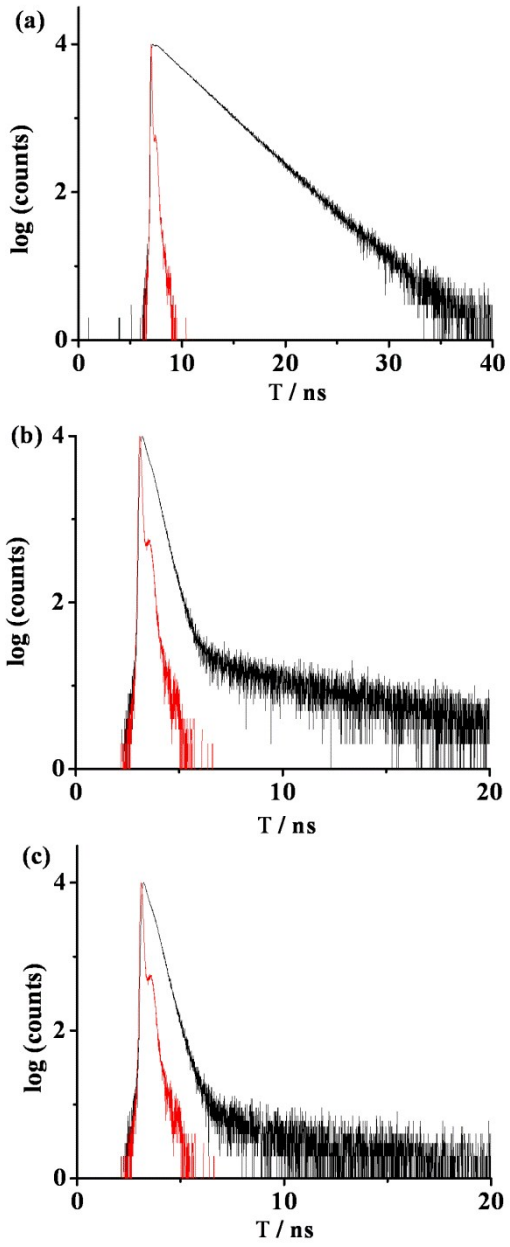

Figure S6. Fluorescence decay profiles of (a) **1**, (———); λem = 676 nm, (b) **2**, (———); λem = 654 nm, and (c) **3**, (———); λem = 661 nm. The black line represents experimental data, whereas the red line represents best fit.

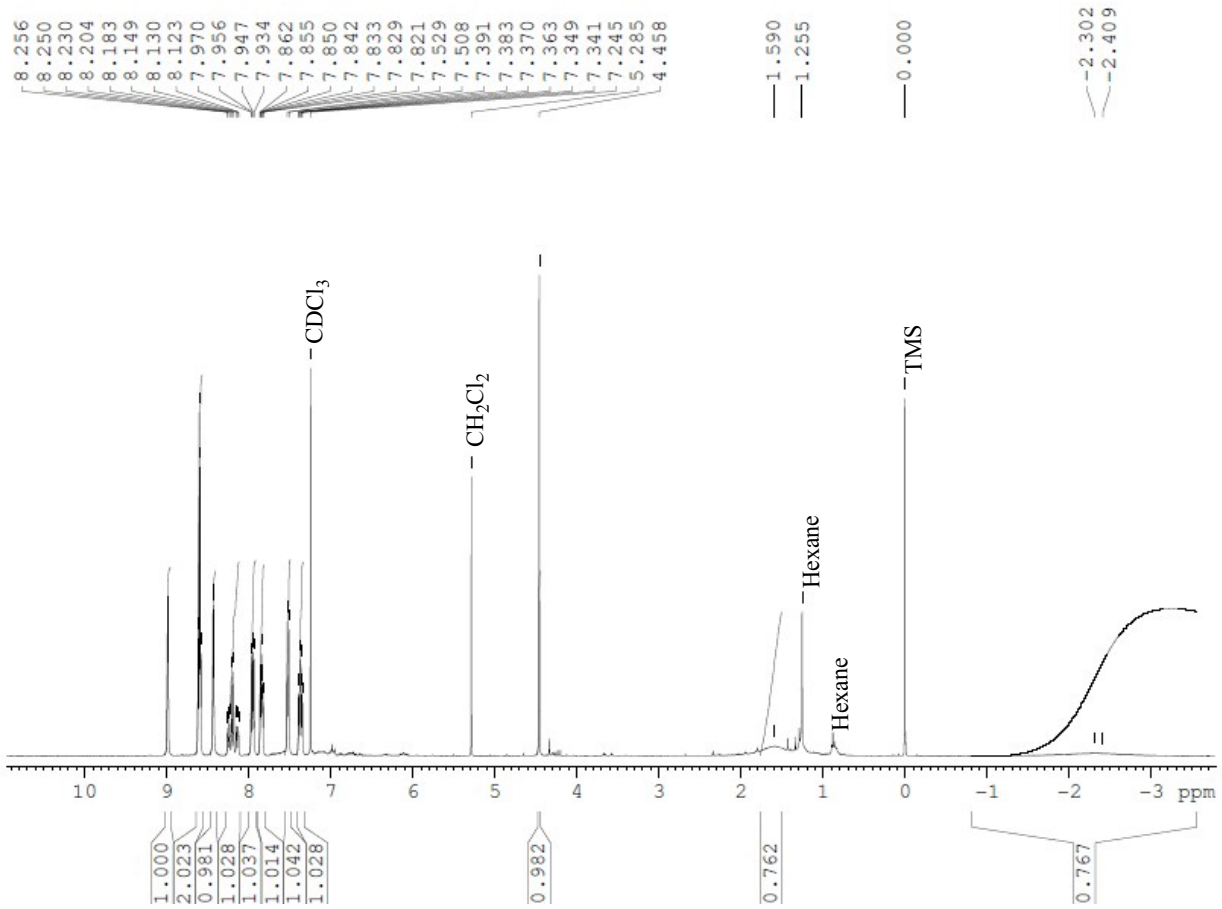

Figure S7. ^{1}H NMR spectrum of 10-[4-(chloroacetoxy)phenyl]-5,15-bis(2-bromo-5-fluorophenyl) corrole, **2**, in $CDCl_3$.

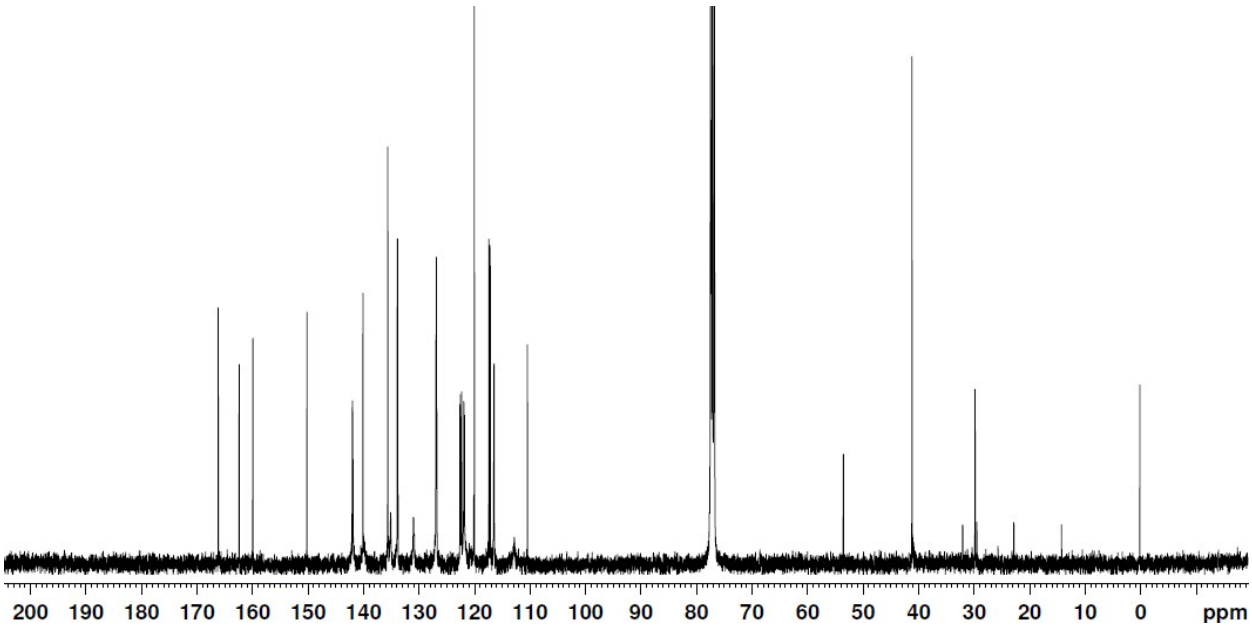

Figure S8. ^{13}C NMR spectrum of 10-[4-(chloroacetoxy)phenyl]-5,15-bis(2-bromo-5-fluorophenyl) corrole, **2**, in $CDCl_3$.

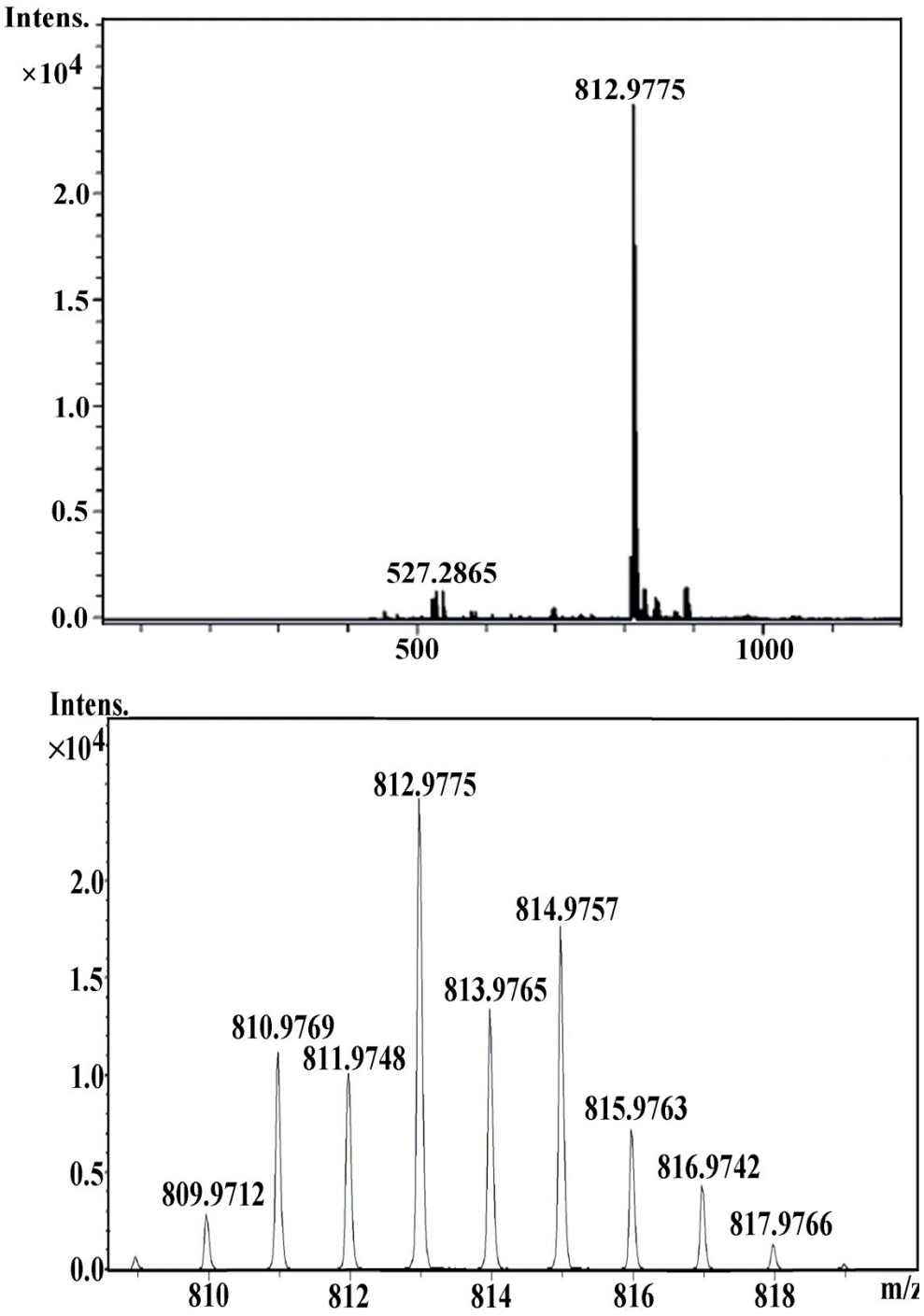

Figure S9. ESI- MS spectrum of 10-[4-(chloroacetoxy)phenyl]-5,15-bis(2-bromo-5-fluorophenyl) corrole, **2**, in CH_3CN shows the measured spectrum with isotopic distribution pattern.

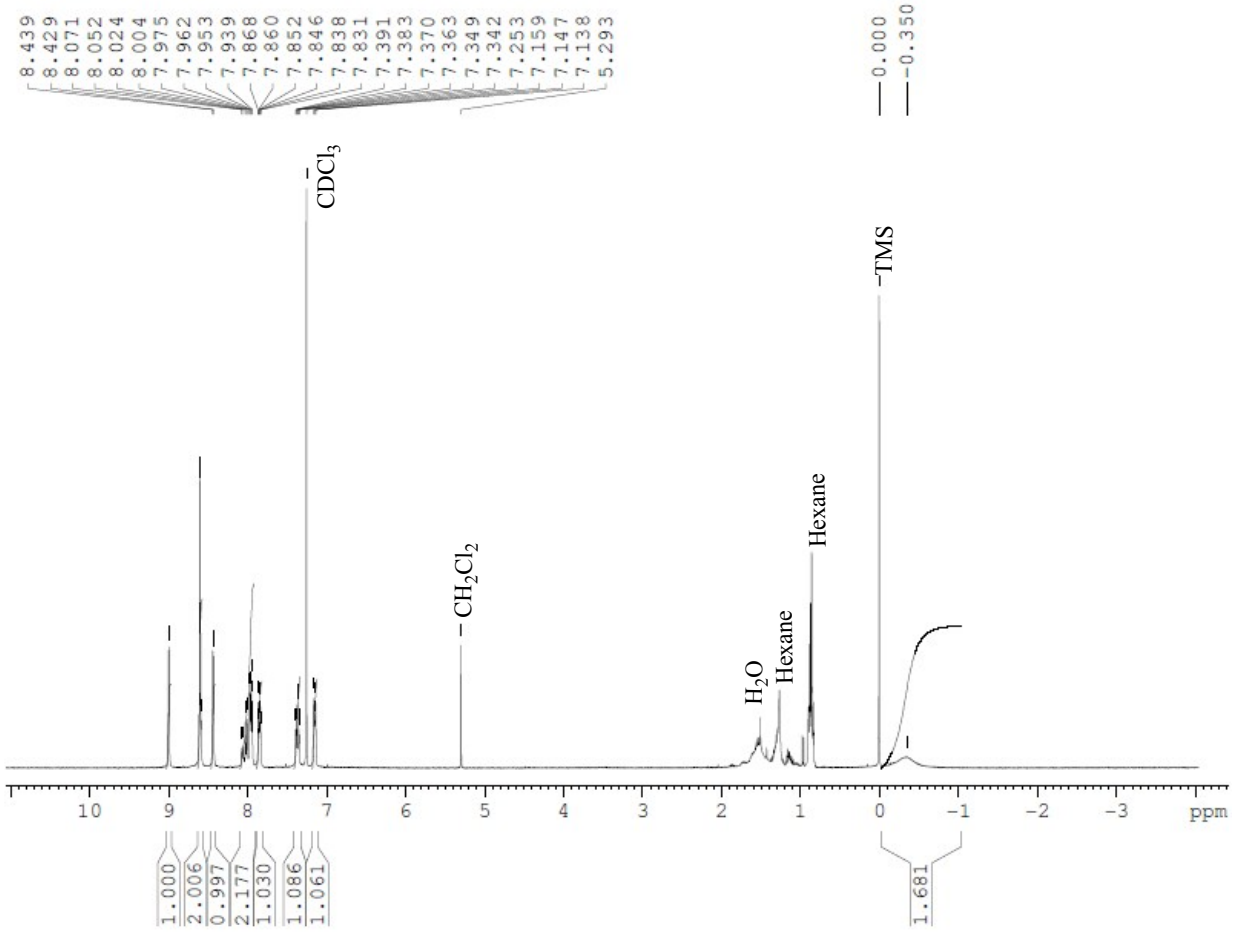

Figure S10. ^{1}H NMR spectrum of 10-(4-hydroxyphenyl)-5,15-bis(2-bromo-5-fluorophenyl) corrole, **3** in $CDCl_3$.

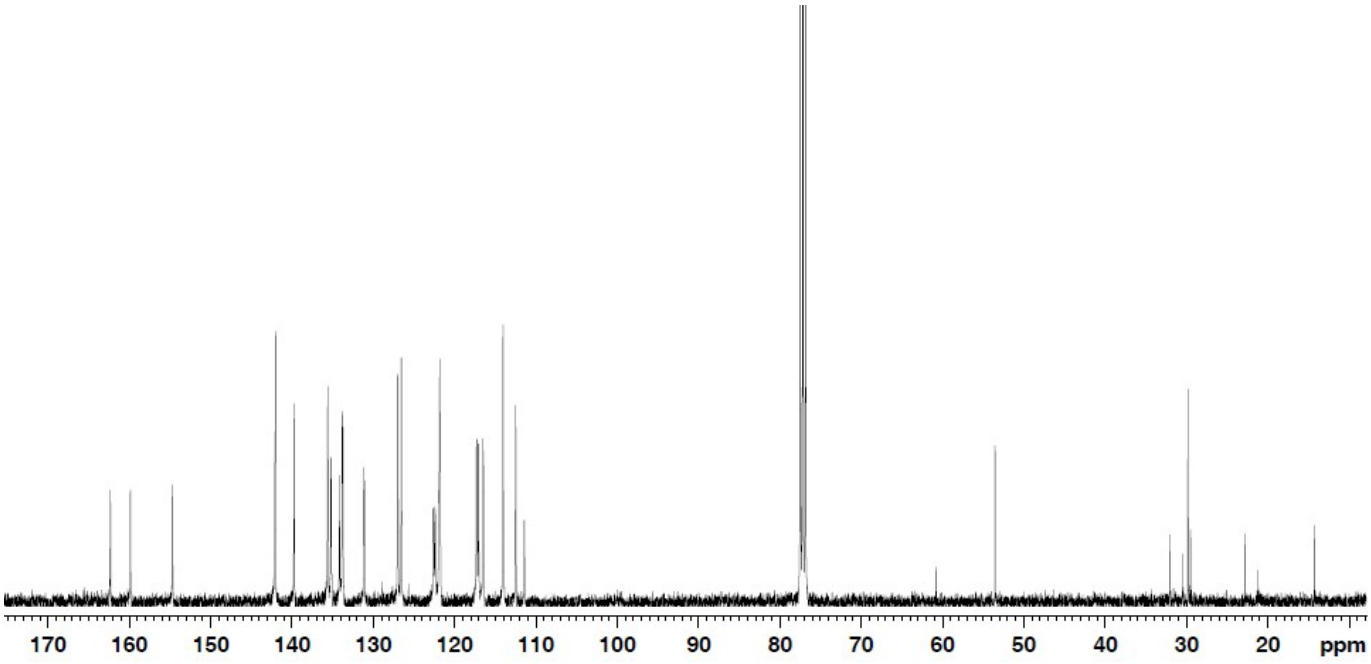

Figure S11. ^{13}C NMR spectrum of 10-(4-hydroxyphenyl)-5,15-bis(2-bromo-5-fluorophenyl) corrole, **3** in $CDCl_3$.

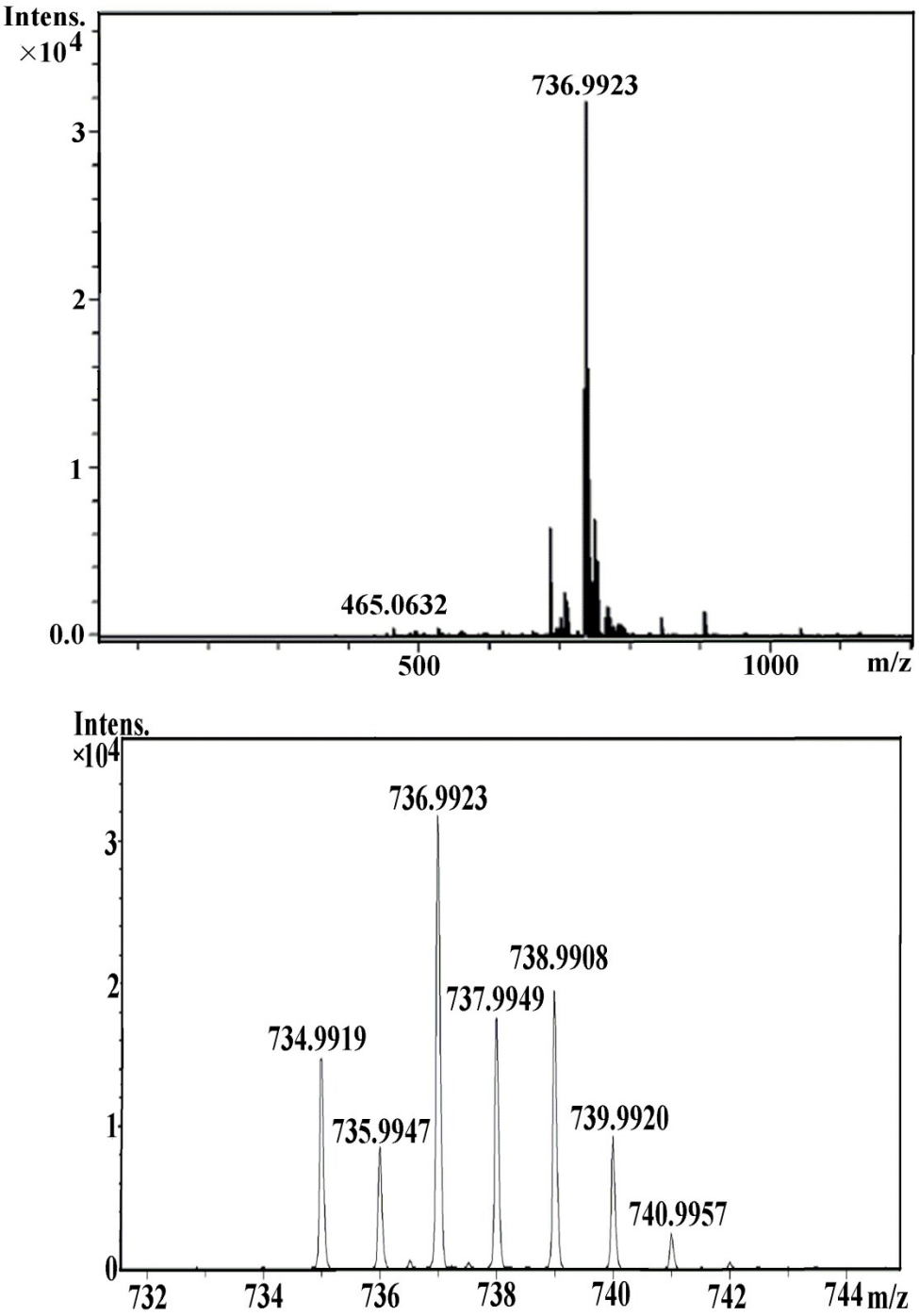

Figure S12. ESI- MS spectrum of 10-(4-hydroxyphenyl)-5,15-bis(2-bromo-5-fluorophenyl) corrole, **3** in CH_3CN shows the measured spectrum with isotopic distribution pattern.

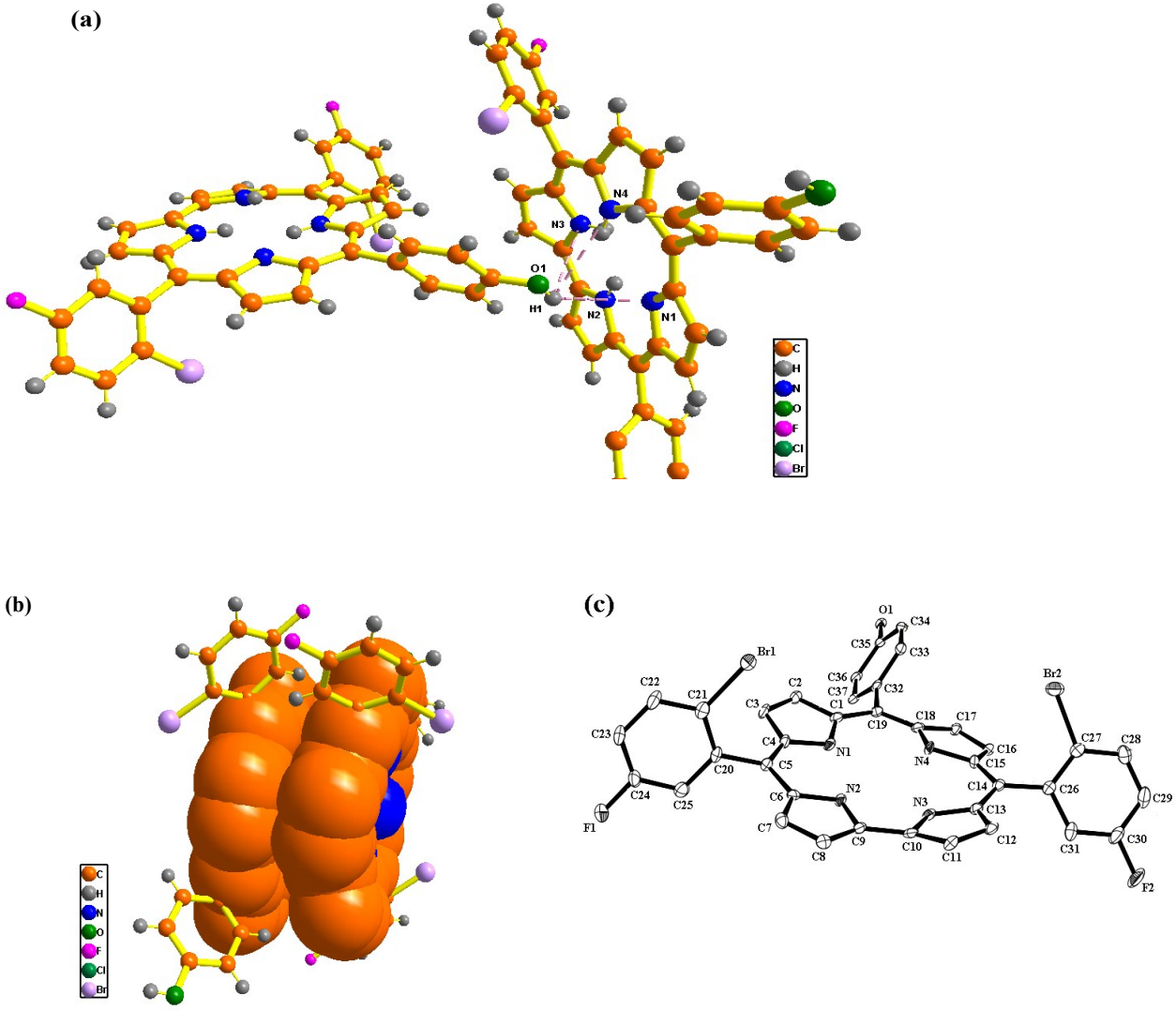

Figure S13. X-ray single crystal structure analysis of 10-(4-hydroxyphenyl)-5,15-bis(2-bromo-5-fluorophenyl) corrole, **3**, (a) O─H...N interactions, [2.86 Å] (b) π- π stacking interactions [3.51 Å]. The entries in square brackets are the distances. (c) ORTEP diagram of **3**. Solvent molecules are removed for clarity. Ellipsoids are drawn at 30% probability.

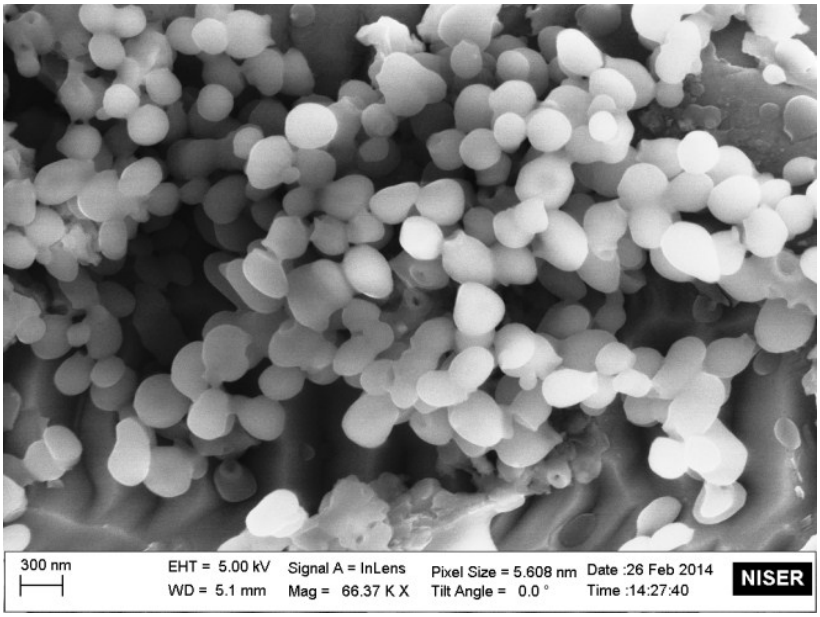

Figure S14. SEM images of the **1** in dichloromethane ─ methanol mixture; nanospheres are seen.

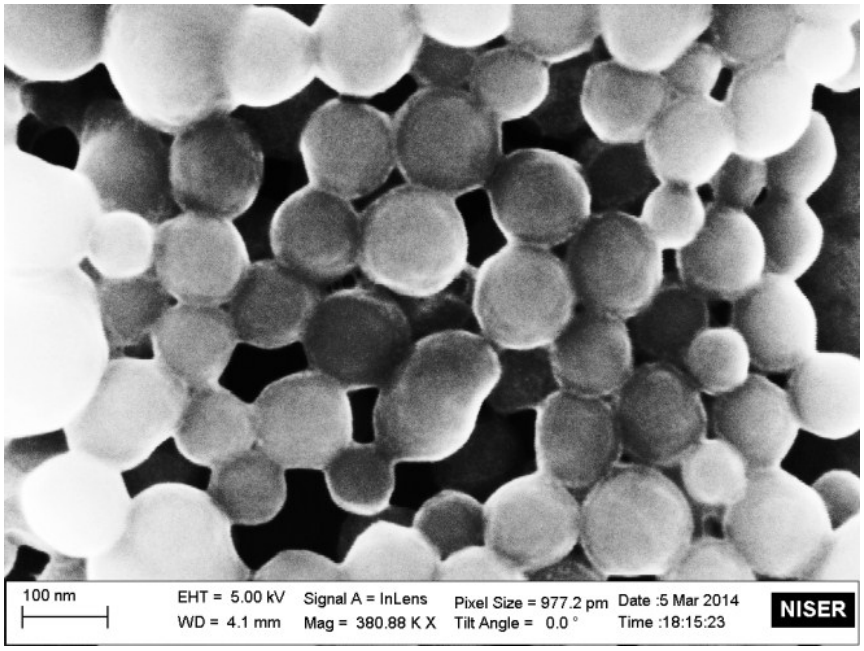

Figure S15. SEM images of the **3** in dichloromethane ─ methanol mixture; nanodiscs are seen.

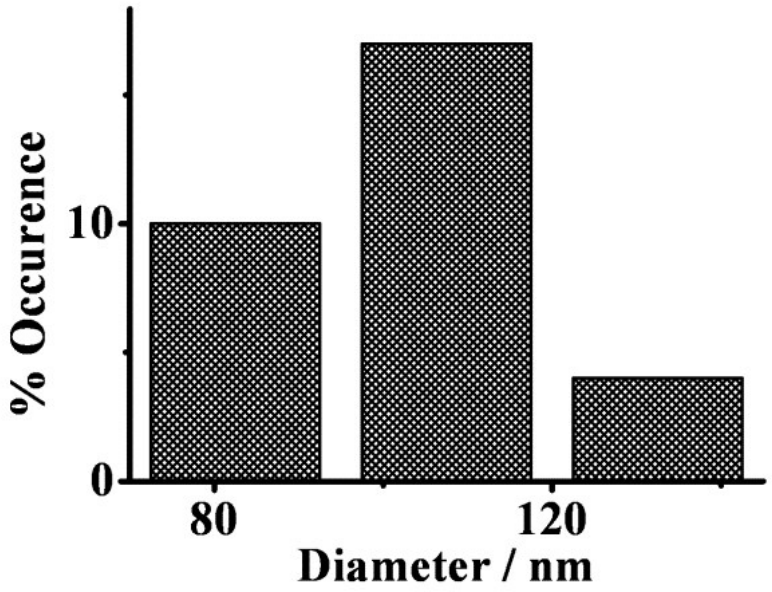

Figure S16. Particle size distribution histograms of nanodiscs of **3**.

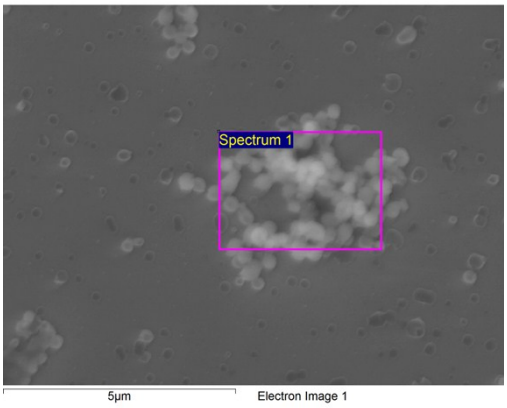

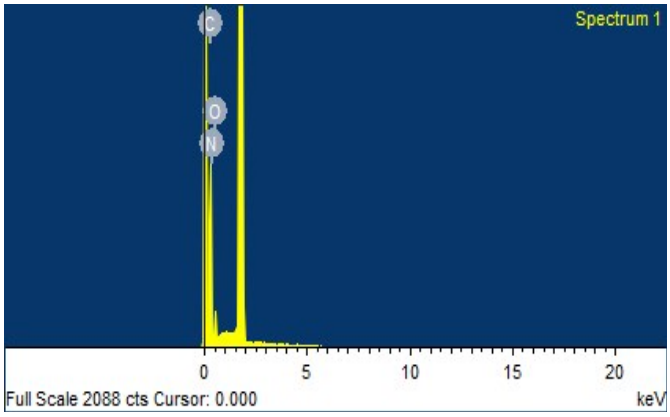

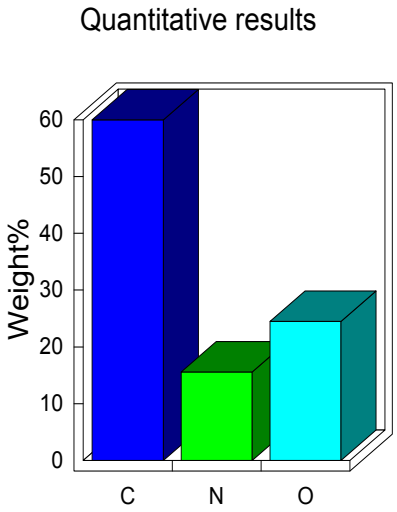

Element	Weight%
C K	59.95
N K	15.59
O K	24.46
Totals	100.00

Figure S17. EDX elemental analysis obtained from the nanospheres of **1** showing the presence of the entire constituent elements: C, N, and O.

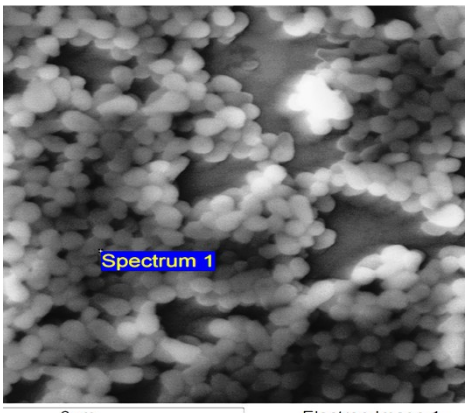

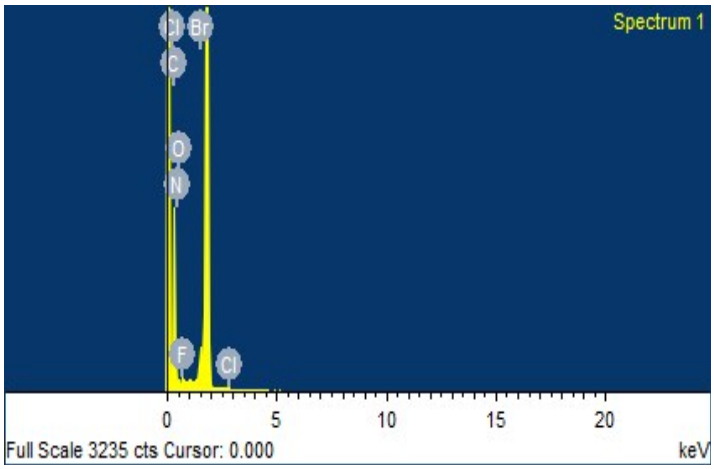

Quantitative results

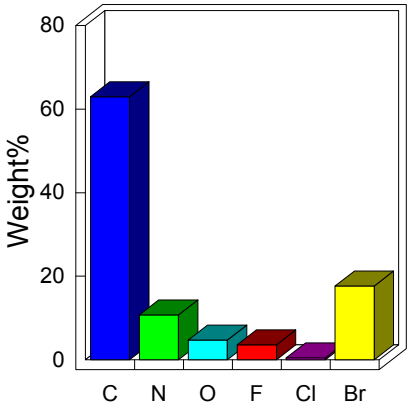

Element	Weight%
C K	62.92
N K	10.70
O K	4.69
F K	3.57
Cl K	0.47
Br L	17.65
Totals	100.00

Figure S18. EDX elemental analysis obtained from the nanobulbs of **2** showing the presence of the entire constituent elements: C, N, O, F, Cl, and Br.

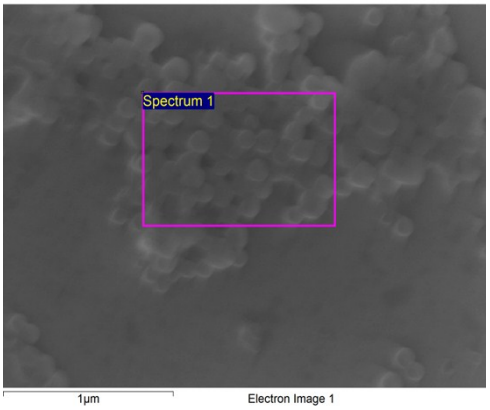

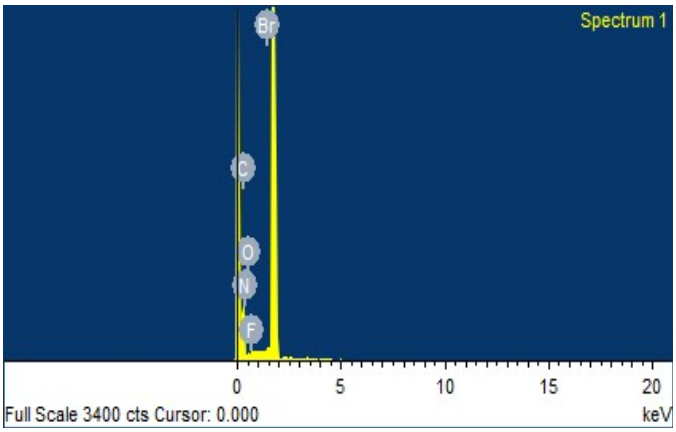

Quantitative results

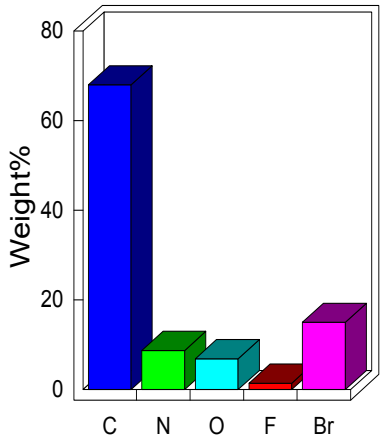

Element	Weight%
C K	67.98
N K	8.73
O K	6.89
F K	1.41
Br L	14.99
Totals	100.00

Figure S19. EDX elemental analysis obtained from the nanodiscs of **3** showing the presence of the entire constituent elements: C, N, O, F, and Br.

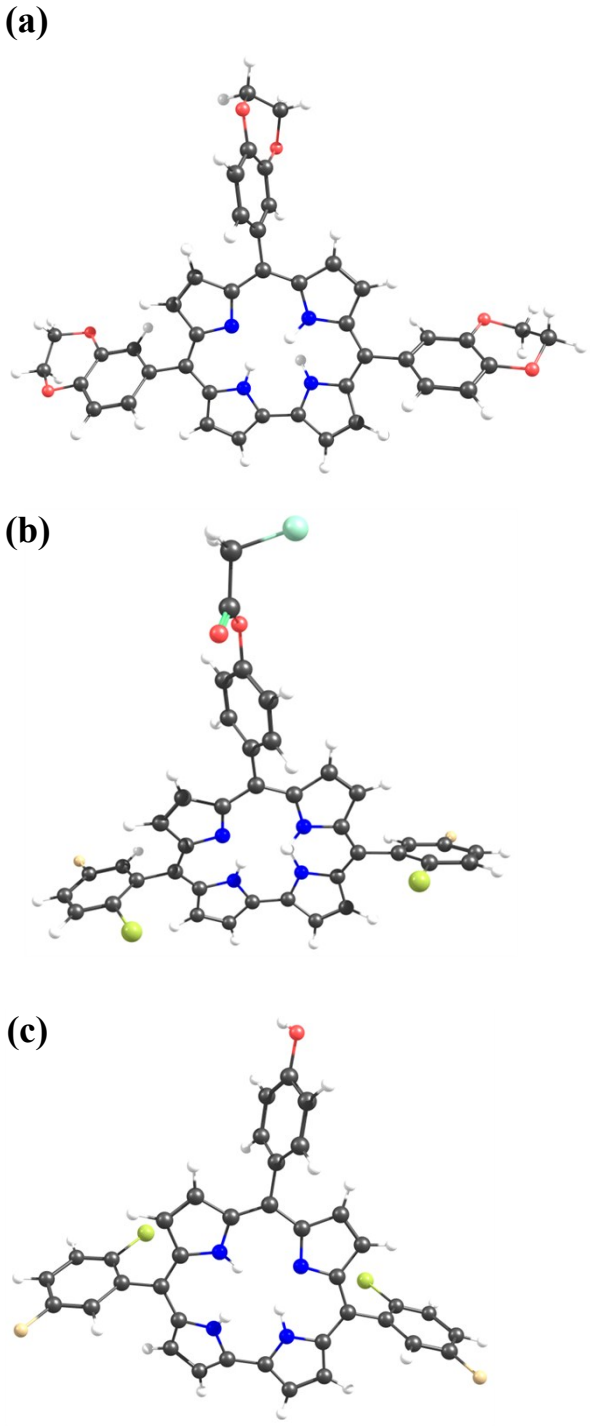

Figure S20. DFT optimized (BP-86/TZVP) structures of (a) **1**, (b) **2**, and (c) **3**.

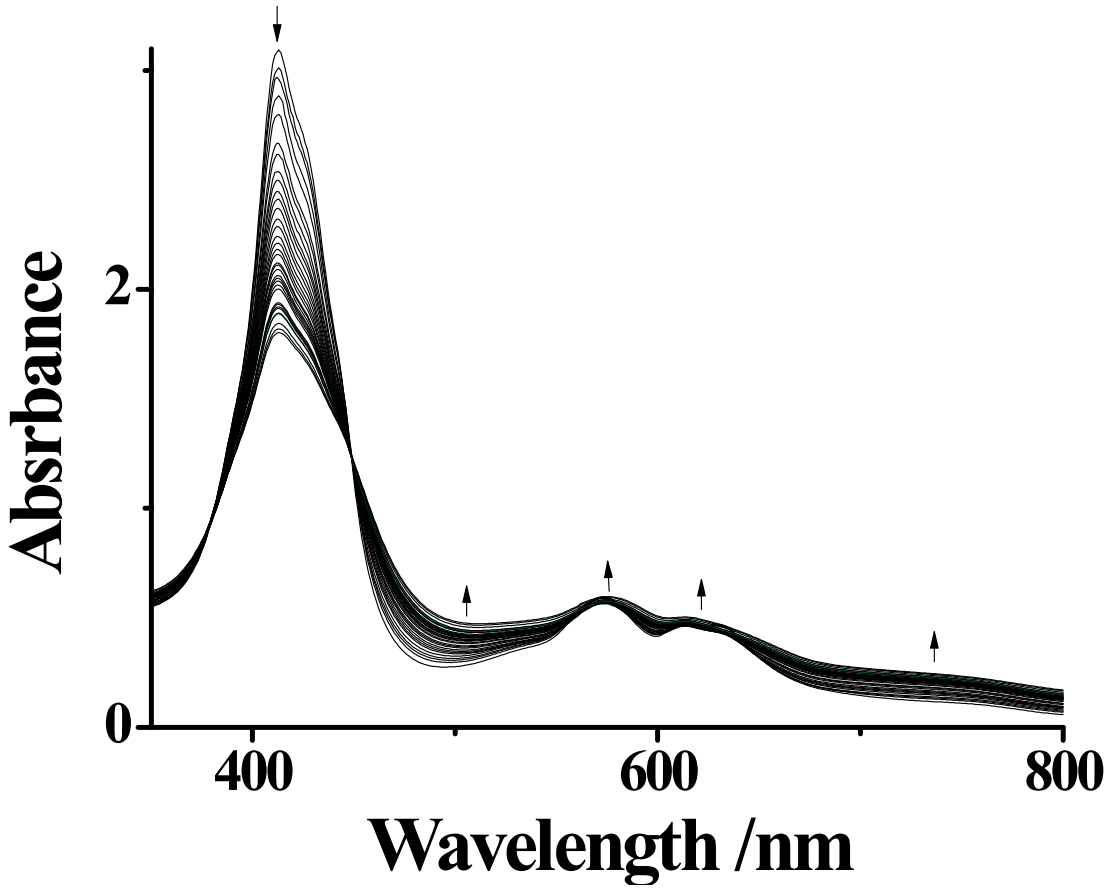

Figure S21 Changes in the UV-Vis spectrum of **3** on letting it stay in a DMF and H_2O (1:1) mixture. Measurements are made at 10 minutes interval.

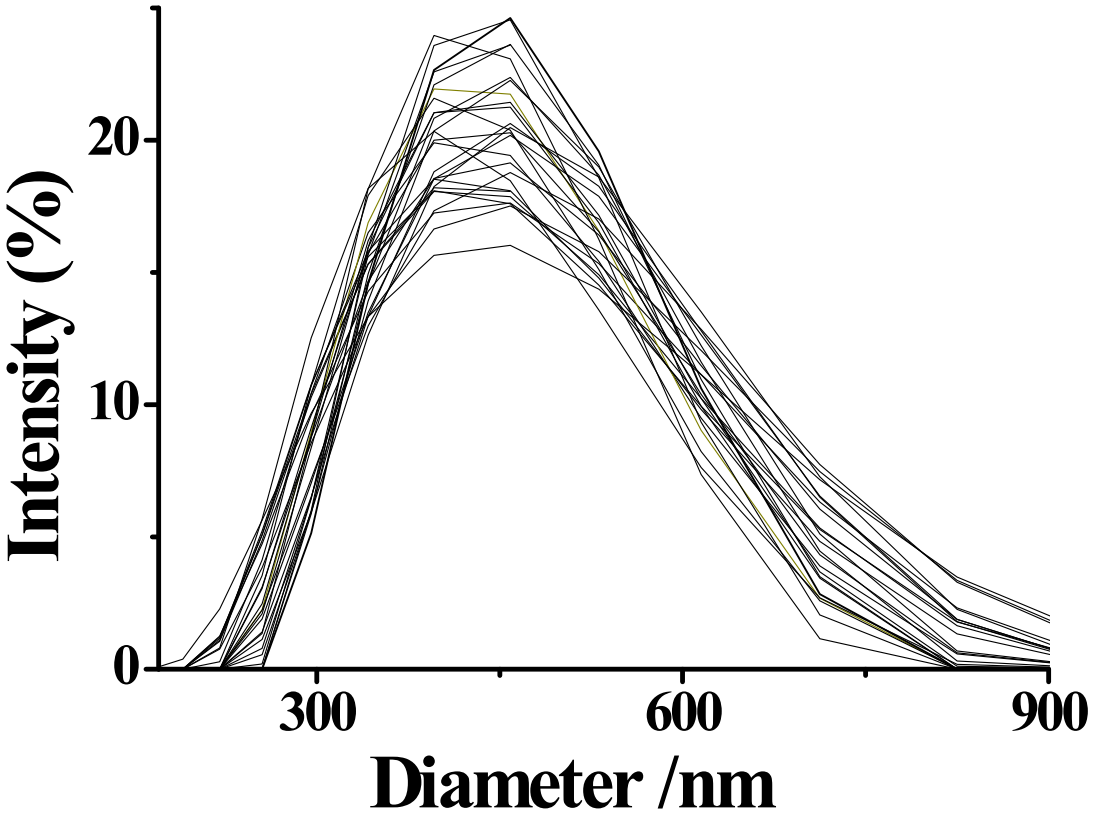

Figure S22 Changes in particle size distribution of the aggregates of **3** on letting it stay in a DMF and H_2O (1:1) mixture. Measurements are made at 10 minutes interval.

Table S1 σ_{TPA} values for related compounds

Compound	Solvent	Method	n_2	σ_{TPA}	Ref.
TTC	CH_2Cl_2	Z-scan	-60×10^{-16} (cm^2/W)	1408-5410 GM	16
TPC	CH_2Cl_2	Z-scan	-100×10^{-16} (cm^2/W)	2301-2576 GM	16
PTTC	CH_2Cl_2	Z-scan	-5.1×10^{-16} (cm^2/W)	233-543 GM	16
GeTTC	CH_2Cl_2	Z-scan	-7.6×10^{-16} (cm^2/W)	112-239 GM	16
A_3-Corroles	CCl_4			130 ± 26 GM	15
DH_3CD	CH_2Cl_2	Z-scan		1100 GM	54
DH_2CD	CH_2Cl_2	Z-scan		3700 GM	54
DZnCD	CH_2Cl_2	Z-scan		4600 GM	54
H_2TPP	Toluene			1-25 GM	55
1a	$CHCl_3$			56 (8) GM	56
1b	$CHCl_3$			187 (62) GM	56
CuTPP	$CHCl_3$			101 (32 GM	56
PEP	$CHCl_3$			<5 GM	56
AF-250	$CHCl_3$			30 GM	56
BDPAS-porphyrin dyad	Different Solvents			1000 GM	57
4D	$CHCl_3$			370 GM	58
5D	$CHCl_3$			7600 GM	58
5M	$CHCl_3$			1800 GM	58
7M	$CHCl_3$			1200 GM	58
8	$CHCl_3$			1000 GM	58
Porphycenes	$CHCl_3$	Z-scan		$8-21\times10^3$ GM	59
1	Toluene	Z-scan	16.8×10^{-18} (m^2/W)	5.7×10^{-12} m/W	This work
2	Toluene	Z-scan	7.8×10^{-18} (m^2/W)	1.9×10^{-12} m/W	This work
3	Toluene	Z-scan	25.9×10^{-18} (m^2/W)	17×10^{-12} m/W	This work
1-nano	–	Z-scan	1.1×10^{-15} (m^2/W)	4.0×10^{-10} m/W	This work
2-nano	–	Z-scan	1.9×10^{-15} (m^2/W)	2.0×10^{-10} m/W	This work
3-nano	–	Z-scan	71.8×10^{-15} (m^2/W)	444×10^{-10} m/W	This work